

The study of the spatial structure of a wake behind a sphere is one of the traditional problems of hydrodynamics. Various visualization methods have shown that the pattern of the satellite flow directly behind a sphere in a homogeneous liquid has axial symmetry over a wide range of Reynolds numbers ($Re < 10^5$). Even upon loss of stability in the main flow, formation of turbulent filaments and loops which destroy the axial symmetry of the flow occurs at some distance from the body [1-4]. The turbulent structure of a wake behind a sphere in a stratified liquid was visualized in [5-10]. To distinguish individual details of the flow a soluble dye was deposited on the sphere surface in the vicinity of the forward braking point [5], and was also introduced in thin horizontal layers as the basin was filled [7] and in vertical columns (markers) before beginning the experiments. Traditional techniques using dye, hydrogen bubbles, introduced particles, and spatial shadow (Schlieren) methods [8, 9, 10] do not permit recording those elements of the wake spatial pattern due to factors such as shading, integration over the ray path, or methodologically restricted viewing direction. It is usually assumed that weak stratification has no effect on the flow pattern, the wake in the immediate vicinity of a sphere in a medium of inhomogeneous density being bounded by a cylindrical turbulent curtain and there existing a stratified flow structure about the sphere similar to the flow structure of a homogeneous liquid. The goal of the present study is to investigate the spatial structure of the satellite flow behind a sphere moving in uniform horizontal motion in an exponentially stratified medium, in particular, to visualize the flow detachment line.

The dimensional parameters of the problem are U , the velocity of the motion, d , the sphere diameter, $\rho(z)$, the liquid density (the z -axis being vertical), g is the acceleration of gravity, ν is kinematic viscosity, k_s , salt diffusion coefficient (the factor creating stratification), and $\Lambda = \left(\frac{1}{\rho} \left| \frac{d\rho}{dz} \right| \right)^{-1}$, the stratification scale. Together with the scale Λ the amount of stratification is often characterized by the buoyancy period (frequency N) $T_k = 2\pi/N = 2\pi\sqrt{\Lambda/g}$, which is independent of depth in an exponentially stratified medium. The basic dimensionless parameters of the problem are the Reynolds number $Re = Ud/\nu$, the internal Froud number $Fr = U^2\Lambda/gd^2 = U^2/N^2d^2 = U^2\rho_0/gd\Delta\rho$, the scale ratio $C = \rho_0/\Delta\rho = \Lambda/d$ and the Schmidt number $Sc = \nu/k_s$ (ρ_0 is the density on the body motion horizon, $\Delta\rho \approx \rho_0 d/\Lambda$, is the density variation over a distance d in the case of weak stratification). Usually the Schmidt number is not included among the defining parameters. However some stable features of the stratified satellite flow pattern show that the difference of the kinetic coefficients in the liquid ($\nu \neq k_s$, $Sc \gg 1$) is significant, and the cause of important elements of the flow structure absent in principle in a homogeneous liquid.

The experiments were performed in rectangular basins $0.7 \times 0.25 \times 0.7$ m and $2.4 \times 0.4 \times 0.6$ m in size, filled with a depth-stratified table salt solution. To estimate the effect of the inhomogeneity in the original stratification on the pattern of flow about the body two filling methods were used - layered, and continuous escape [11]. The depth distribution of the buoyancy period was measured to an accuracy of 5% by optical and probe methods using a density marker formed behind a vertically ascending gas bubble [12]. The sphere was towed at constant velocity by a 0.5-mm diameter guide passing through its center. A second conductive filament was placed parallel to the guide at a distance of 1 mm. The velocity and stability of the motion were monitored by the measured frequency of rotation of a disk with orifices, installed on the drive drum. Uncertainty in velocity measurement did not exceed 1%. Transparent polished Plexiglass spheres 3.0 and 5.0 cm in diameter were used. The interval between individual experimental was less than 3-4 hr. Over such a time period all dynamic and density perturbations established by the initial density gradient damped out.

The experiments performed indicated that the filling method had no effect on the flow pattern elements studied: both layered (with regular density perturbation distribution over depth) and continuous (with random distribution) methods were used. The flow pattern was maintained in both basins and did not depend on the orientation of the sphere trajectory relative to the side walls of the basin. Flow visualization was carried out by the traditional shadow method (using a Foucault knife-edge as the vertical slit), the inclined slit method, and the colored shadow method. However the body (transparent or opaque) shades the shadow picture and does not allow determination of the form of the flow detachment lines. In the traditional shadow method the ray of light enters the medium horizontally, which eliminates the possibility of detecting individual elements and identifying any three-dimensional structure.

In addition to the traditional methods the electrolytic visualization method employed in [13] to display the flow structure in the wake behind a sphere in a homogeneous liquid was used. This method is based on anodic oxidation of tin, lead, and their alloys under the action of a dc electric current. Highly dispersed products of tin oxidation are formed on the anode surface in the salt solution - particles $\sim 1 \mu\text{m}$ in size, consisting of tin monoxide and dioxide, tin dichloride, and stannic acids. Qualitatively, this method is similar to flow visualization using smoke in aerodynamic tubes. The suspension formed at the anode surface ("white smoke") produces photographic contrast and allows use of traditional photorecording methods, while at the same time it is sufficiently transparent to permit simultaneous observation of the forward and back (along the line of sight) boundaries of the flow. By changing the form and relative position of the anode, various portions of the film can be colored. The second electrode (cathode) was a brass bar, installed parallel to the line of motion of the body at a distance of 15 cm. Different anode forms were used in the experiments. An annular belt 3 mm wide was installed vertically flush on the equator of the sphere surface, in a vertical plane perpendicular to the line of motion. Also used was a vertically oriented half-ring passing through the forward (rear) braking point, and a sphere segment 15 mm in diameter encompassing the line of motion. The clearest flow patterns were produced with the ring electrode. The "white smoke" uniformly departing from the ring was clearly visible on the surface of the polished transparent Plexiglass sphere and permitted recording the form of the breakaway lines and the wake boundary in both the direct vicinity of the body and at large distances therefrom.

It should be noted that the density of the tin compound particles is higher than the density of the salt solution on the body motion horizon. In a homogeneous liquid the cylindrical curtain behind the sphere uniformly sank at a slow rate, and its axis did not coincide with the trajectory of the horizontal motion of the sphere center. In the stratified liquid the suspension remained on the motion horizon at all visualization times. Sinking of the tin compound particles was observed only on the sphere surface and led to more intense coloration of the lower portion of the wake. The flow pattern was recorded with a Zenit-TTL camera (focal length $f = 58 \text{ mm}$, speed 1:2) using 7 and 14 mm extension tubes. The photographs were taken against a dark background with lateral lighting by a Foton lamp (electrical power 500 W), with angle of view being $40\text{-}50^\circ$ from the vertical. To decrease the rate of solution of the visualization band and preserve the form of the sphere, the current was switched on only when the body moved through the camera's field of view.

To monitor the operation of the technique the satellite flow pattern behind a uniformly moving sphere in a homogeneous liquid was visualized first. The experiments were performed in a table salt solution of constant concentration having a density of $\rho_0 = 1.014 \text{ g/cm}^3$. A typical flow pattern is shown in Fig. 1 ($d = 5 \text{ cm}$, $U = 0.7 \text{ cm/sec}$, $Re = 350$). In this regime an axisymmetric bottom vortex is formed behind the body, and in the photograph one can clearly see the converging cylindrical axisymmetric curtain, the back edge of which is twisted into a ring vortex which generates a secondary curtain. With change in Re the turbulent curtain may change into a pair of rectilinear or twisted turbulent filaments [14] or into three-dimensional turbulent loops [3, 13]. In all cases in the immediate vicinity of the sphere before the onset of instability in the satellite flow, leading to formation of secondary turbulent bands or loops, the curtain retains axial symmetry. One can clearly see the line of detachment from the sphere - a circle, the position of which on the body depends on the Reynolds number Re .

Relatively weak stratification ($C = \Lambda/d = 125 \gg 1$, $\Delta\rho/\rho_0 = 8 \cdot 10^{-3} \ll 1$, where $\Delta\rho$ is the difference in the densities of the medium in horizontal planes passing through the upper- and lowermost points of the sphere, ρ_0 is the density of the liquid at the level of the sphere center) leads to a qualitative change in the satellite flow pattern - the wake loses

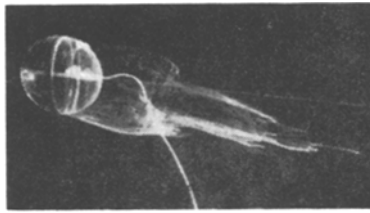


Fig. 1

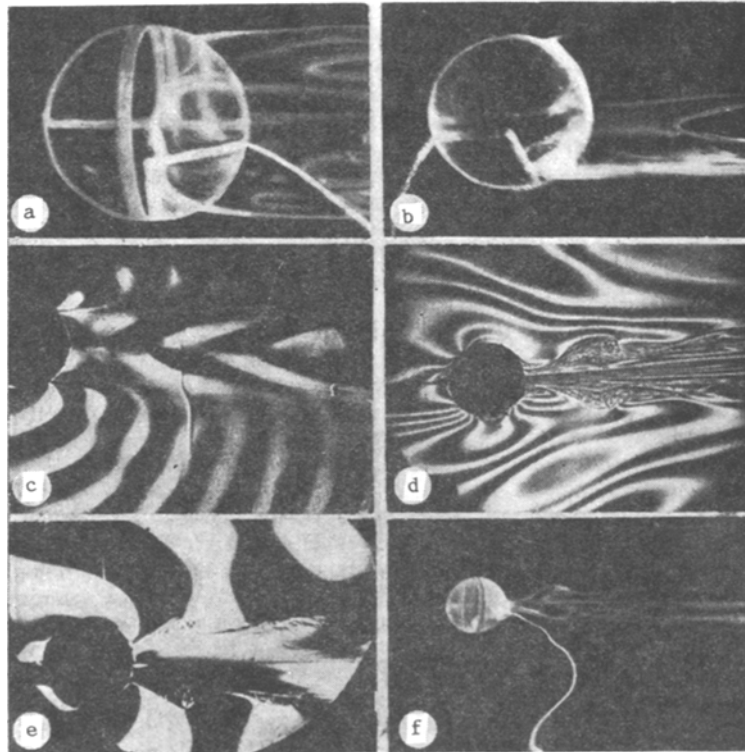


Fig. 2

axial symmetry. A typical pattern of flow in a stratified liquid is shown in Fig. 2a (the sphere with $d = 5$ cm moves to the right, $U = 0.7$ cm/sec, $Re = 350$, $Fr = 0.012$). The suspension departing uniformly from the tin ring is redistributed along the detachment line and clearly distinguishes four planar arcs of that line, two of which lie in a horizontal plane, and two, in the vertical. The coloration is intensified in the vicinity of the lines of intersection of the horizontal and vertical turbulent layers forming the shell of the wake (in the photograph one can also see the drive rod passing through the channel into the body of the sphere to the visualization electrode). In Fig. 2a a second vertical breakaway line can be seen through the transparent sphere on its far side.

The corresponding flow pattern on which arrows denote the trajectory of particles departing from the ring, the detachment line, and the contour of the dyed wave shell is shown in Fig. 3a. According to many visual observations and stereophotographs the suspension was uniformly distributed over the sphere surface between the visualization band and the breakaway line, and is concentrated in the vicinity of the three-dimensional piecewise-continuous breakaway line, consisting of four arcs of circles. The two arcs AB and CD lie in a horizontal plane, while AC and Bd lie in vertical planes. The width of the inclined transition region in the vicinity of points A, B, C, D depends on the degree of homogeneity of the initial density gradient. A change in symmetry upon breakaway of the flow was observed in experiments with a different visualization belt configuration. These features of the wake structure reflect the interaction of the turbulent motion within the wake and the external flow. They appear most clearly in observations of a suspension formed on a vertical half-ring on the downstream portion of the sphere (Fig. 2b).

The corresponding flow pattern is shown in Fig. 3b. Here EF is the equatorial half-ring on the downstream portion of the sphere, and the arrows denote particle trajectories.

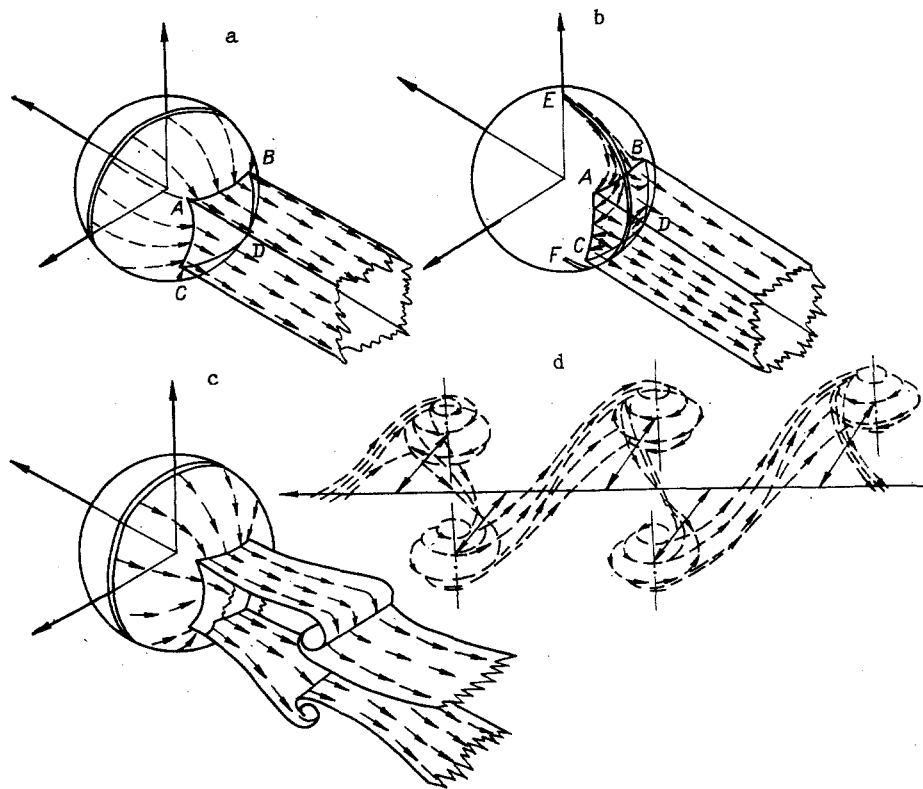


Fig. 3

The suspension in the upper and lower portions of the sphere in the region of detachment-free flow sinks (rises) along the semicircle on the surface, detaches in the vicinity of the horizontal detachment lines AB and CD, and concentrates at their ends in the region of contact with the corners of the wake section contour. The curtain formed within the detachment region in the back flow region (on the portion of the half-ring located between lines AB and CD) spreads to the sides along horizontal isopycnic surfaces, and does not detach from the sphere surface until it reaches the vertical detachment lines AC and BD.

Both the horizontal and vertical turbulent layers departing from the detachment lines (lines of convergence of the external and internal reverse flow regions within the wake) are fronts - thin layers with abrupt density gradients. They separate the liquid flowing over the sphere and the liquid within the wake, in which the density distribution differs significantly from the original. Convergence of the flow leads to increase in concentration of the suspension in the vicinity of the detachment line. Liquid particles in contact with the sphere surface in the detachment and detachment-free flow become concentrated on the outer shell of the density wake. Because of slippage of the heavy suspension along the body surface the lower horizontal portion of the wake shell in Fig. 2b is colored more intensely than the upper. Nonuniformity in the coloration distribution along the lower boundary of the wake indicates the turbulent character of the flow inside the wake.

It follows from all the experiments performed with electrolytic visualization that relatively weak stratification leads to a qualitative change in the structure and symmetry of the satellite flow behind the sphere. Continuous axial symmetry of the flow in the homogeneous liquid is replaced by discreteness. The wake in the stratified liquid is symmetric relative to vertical and horizontal planes passing through the line of body motion. The change in the character of symmetry indicates the intense effect of weak stratification on the flow pattern. These features of the satellite stratified flow are related to formation on the sphere surface of a thin high-gradient density boundary layer, which intensifies the effect of the weak stratification [15]. Formation of a density boundary layer and splitting of the internal motion scales (difference in the thicknesses of the velocity and density boundary layers) depends on spatial dispersion - noncoincidence of the molecular transport coefficients for momentum (kinematic viscosity) and matter (salt diffusion coefficient) - and indicates the necessity of using a complete system of equations including terms with molecular diffusion in theoretical analysis of flow over a body by a slightly stratified liquid.

Figure 2c, d shows traditional shadow photographs of stratified flow in the wake behind a sphere and a black and white print of a color shadow image. The variations in darkness in Fig. 2c ($d = 5$ cm, $U = 0.78$ cm/sec, $T_k = 3.5$ sec, $Re = 384$, $Fr = 0.0075$) are caused by the horizontal component of the index of refraction (density), while in Fig. 2d ($d = 4$ cm, $T_k = 3$ sec, $U = 1.96$ cm/sec, $Re = 784$, $Fr = 0.055$) they are produced by the vertical component. A large portion of the image is filled by combined internal waves (light and dark semicircles of Fig. 2c). Ahead of the body there is a region of stagnant liquid in which a slow turbulent motion exists. As a result of a "raking" effect: liquid from the horizontal plane of the body's motion enters the blockage region, so that the density gradient therein is less intense than in the unperturbed medium. In Fig. 2d the blockage region lies between the horizontal isophotes ahead of the body. Near the upper and lower poles of the sphere in Fig. 2d one can see intense fine-scale fluctuations in density, related to high-gradient density boundary layers. As it flows away the density boundary layer forms the extremely thin high-gradient shell of the density wake.

In view of the small thickness of this shell its reliable registration requires use of optical methods with high spatial resolution. In the slot-knife and filament at the focus methods a minimum width of the illumination slot (0.2-0.3 mm) is established. The density boundary layer can be detected most conveniently by shadow methods which do not visualize internal waves, for example the inclined slot-filament at the focus technique. Analysis of shadow kinograms of experiments with simultaneous electrolytic visualization shows that the suspension is concentrated primarily in the high-gradient shell of the wake - in horizontal layers and (according to other observations) in vertical fronts. The two successive density markers in Fig. 2c visualize the profile of the horizontal velocity component and illustrate the difference in thickness of layers with velocity shear and high density gradient.

Since the vertical density distributions inside and outside the wake differ from each other, the wake dimensions and configuration can be affected by buoyancy forces. In a number of regimes the wake periodically pulsates along the vertical and spreads in the horizontal direction. The first maximum in the vertical dimension of the wake is found at a crest (valley in the lower semispace) of the combined internal wave at a distance $x \approx 0.5UT_k$ from the body. With increase in body velocity it is in this region that wave-turbulent instability (or Kelvin-Helmholtz instability) begins to develop. A shadow kinogram with characteristic internal bow-wave, indicating development of Kelvin-Helmholtz instability in the region with maximum density gradients, is shown in Fig. 2e ($d = 5$ cm, $T_k = 3.5$ sec, $U = 1.09$ cm/sec, $Fr = 0.049$, $Re = 983$). A picture of this form of flow obtained by electrolytic visualization is shown in Fig. 2f ($d = 3$ cm, $T_k = 11$ sec, $U = 0.6$ cm/sec, $Re = 180$, $Fr = 0.023$). The difference in the contours of the wake boundaries in Fig. 2e, f is also related to scale splitting, which leads to a smoother velocity distribution in the instability zone and a more abrupt change in density and its gradient. The corresponding flow pattern is shown in Fig. 3c. As in the preceding ones, in this regime the color is concentrated primarily in the vicinity of the corner lines formed by intersection of vertical and horizontal high-gradient layers of on the boundary of the wake.

The basic mechanism of stability loss in a satellite flow in a homogeneous liquid is related to accumulation of vorticity on the downstream portion of the sphere and its ejection into the wake in the form of a turbulent curtain, turbulent filaments, or irregular turbulent loops. In addition to this form of stability loss, in a stratified liquid flow instability can also develop in horizontal high-gradient layers (shear or wave-turbulent) and invertical turbulent layers. These forms of instability are characterized by different time and space scales. The longest-lived prove to be turbulent structures generated by vertical turbulent layers. Interaction of flows in vertical turbulent layers leads to their meandering in the horizontal direction and formation of periodic spatial turbulent structures with a vertical axis, the external shell of which is formed by liquid colored by tin compounds. The corresponding flow pattern is shown in Fig. 3d. The trajectories of all colored particles on the upper (lower) boundary of the vortices lie in a single plane, in degenerating horizontal layers with a maximum density gradient. Within the vortices the flow is significantly three-dimensional with particles moving from the periphery to the center of the vortex, and from its upper and lower boundaries to its center. Three-dimensional colored turbulent layers joining individual vortices to each other slowly evolve, forming arbitrarily oriented surfaces of complex form.

In some regimes turbulent dipoles are formed on the side boundaries of the wake - pairs of vortices of opposite sign with a vertical axis of rotation joined by a common shell. Such a configuration drifts slowly, while the individual elements of a given pair may separate and form a common turbulent dipole with a vortex from another dipole. After motion in the liquid degenerates a turbulent structure of the visualization suspension "freezes," moving extremely slowly through the basin and disappearing even more slowly due to molecular diffusion. Just such a form of motion, visually similar to a turbulent bridge in the wake behind a vertical cylinder, has been observed several times previously [5-7]. In other regimes a portion of the vertically oriented shell breaks into layers and sets in motion a body in the form of two plane wedges adjacent to the wake axis.

Because of the difference in characteristic times of formation and existence of turbulent structures the pattern of satellite flow behind a sphere in a stratified medium can change significantly with removal from the body. The degree to which individual elements of the structure are expressed depends on the ratios of the defining parameters - Re , Fr , C , Sc . At moderate distances from the body, vortices with a horizontal axis are more prominent, while at large distances those with a vertical axis are. A thin density boundary layer, which forms the high-gradient shell of the wake, exists in all the regimes of stratified flow over a sphere which were considered.

The authors are indebted to V. V. Tikhomirov for assistance in preparing the experiments.

LITERATURE CITED

1. G. K. Batchelor, *An Introduction to Fluid Dynamics*, University Press, Cambridge (1967).
2. M. Van Dyke, *Album of Liquid and Gas Flows* [Russian translation], Mir, Moscow (1986).
3. E. Achenbach, "Vortex shedding from spheres," *J. Fluid Mech.*, 62, No. 2 (1974).
4. S. Taneda, "Experimental investigation of the wake behind a sphere at low Reynolds numbers," *Repts. Res. Inst. Appl. Mech. Jpn.*, 4, No. 16 (1956).
5. H. D. Pao and T. W. Kao, "Vortex structure on the wake of a sphere," *Phys. Fluids*, 20, No. 2 (1977).
6. S. I. Voropaev and I. A. Filippov, "Turbulent bridge behind a three-dimensional body moving in a stratified liquid," *Mor. Gidrofiz. Zh.*, No. 6 (1985).
7. W. Debler, "The towing of bodies in a stratified fluid," *IAHR Intern. Symp. on Stratified Flows*, Novosibirsk (1972).
8. K. Lofquist and L. Purtell, "Drag on a sphere moving horizontally through a stratified liquid," *J. Fluid Mech.*, 148, 271 (1984).
9. Yu. D. Chashechkin, S. A. Makarov, and V. S. Belyaev, *Combined Internal Waves*, Preprint Inst. Prikl. Mekh. Akad. Nauk SSSR, No. 214 [in Russian], Moscow (1983).
10. E. Ya. Sysoeva and Yu. D. Chashechkin, "Turbulent structure of the wake behind a sphere in a stratified liquid," *Zh. Prikl. Mekh. Tekh. Fiz.*, No. 2 (1986).
11. J. N. Fortuin, "Theory and application of two supplementary methods of constructing density gradient columns," *J. Polym. Sci.*, 44, 505 (1960).
12. V. N. Nekrasov and Yu. D. Chashechkin, "Measurement of velocity and internal oscillation period in liquids by the density marker method," *Metrologiya*, No. 11 (1974).
13. S. Asaka and Y. Oshima, "Shedding vortices from spheres," *Nat. Sci. Rep.*, 28, No. 1 (1977).
14. S. Taneda, "Visual observations of the flow past a sphere at Reynolds numbers between 10^4 and 10^6 ," *J. Fluid Mech.*, No. 1 (1978).
15. Yu. D. Chashechkin, "Internal waves and discrete turbulent structures of free turbulent flows," in: *6th All-Union Conference on Theoretical and Applied Mechanics, Reports* [in Russian], Nauka, Tashkent (1976).